

A Gaussian-2 ab Initio Study of the $[\text{C}_2\text{H}_5\text{S}]^-$ Potential Energy Surface: I. Structures and Energetics of $[\text{C}_2\text{H}_5\text{S}]^-$ Anions and Fragmentation Pathways of the Thioethoxide Anion

S.-W. Chiu*

Department of Molecular and Integrative Physiology and Beckman Institute for Advanced Studies,
University of Illinois, 405 N. Mathews, Urbana, Illinois 61801

Wai-Kee Li*

Department of Chemistry, The Chinese University of Hong Kong, Shatin, N.T., Hong Kong

Received: January 7, 2001; In Final Form: March 14, 2001

The thermochemical data for the five isomers/conformers of $[\text{C}_2\text{H}_5\text{S}]^-$, $\text{CH}_3\text{CH}_2\text{S}^-$ (**1**), CH_3CHSH^- (**2/3**), and $\text{CH}_3\text{SCH}_2^-$ (**4/5**) have been calculated and compared with available experimental data. The structural and electronic properties of the isomers/conformers are also discussed. Contrary to its oxygen analogue, the 2-mercaptoethyl anion ($\text{HSCH}_2\text{CH}_2^-$) is unstable with respect to the dissociation to $\text{HS}^- + \text{C}_2\text{H}_4$ without an energy barrier. In addition, plausible elimination pathways and intramolecular rearrangements for **1** have also been studied. The 1,2- H_2 elimination $\mathbf{1} \rightarrow \text{H}_2 + \text{CH}_2\text{CHS}^-$ and the 1,2- HS^- elimination $\mathbf{1} \rightarrow \text{HS}^- + \text{C}_2\text{H}_4$ have the lowest-energy barriers (260–267 kJ mol^{-1}) among the plausible elimination reactions of **1** under investigation. Rearrangement $\mathbf{1} \rightarrow \mathbf{3}$ has an energy barrier of 259 kJ mol^{-1} and is energetically competitive with the aforementioned 1,2-elimination reactions. On the other hand, conversion of **1** to **4/5** may proceed via a dissociation and recombination mechanism. The estimated energy cost for $\mathbf{1} \rightarrow \mathbf{4/5}$ is ca. 285 kJ mol^{-1} .

1. Introduction

There have been extensive collision-activated dissociation (CAD) studies of alkoxide anions (RO^-).^{1–7} Bowie and co-workers^{8,9} investigated the mechanism of the elimination reactions of ethoxide and *t*-butoxide with isotope effect experiments and ab initio calculations. The technique of infrared multiple photon (IRMP) photochemistry has also been applied to study the mechanism of fragmentation of alkoxides.^{10,11} All these studies indicate that loss of H_2 or CH_4 (or alkane) from alkoxide is a stepwise 1,2-elimination via an ion–molecule complex (IM-C)¹² as an intermediate.^{8–11} In particular, the gas-phase decomposition of ethoxide ($\text{CH}_3\text{CH}_2\text{O}^-$) has been well studied by both CAD¹ and IRMP¹⁰ methods. A high-level theoretical study on the isomerizations of $[\text{C}_2\text{H}_5\text{O}]^-$ anions and unimolecular fragmentation of ethoxide has recently been reported.¹³ On the other hand, the corresponding sulfur analogues, $[\text{C}_2\text{H}_5\text{S}]^-$ anions, as well as other thioalkoxides (RS^-), have received little attention.

In this work, we study the structures and energetics of the $[\text{C}_2\text{H}_5\text{S}]^-$ anions as well as the fragmentation pathways and intramolecular rearrangements of thioethoxyl anion (**1**), which is the most stable isomer of the $[\text{C}_2\text{H}_5\text{S}]^-$ anions under investigation. The isomerization and fragmentation pathways for 1-mercaptoethyl (**2/3**) and methylthiomethyl (**4/5**) anions will be dealt with in a separate report.¹⁴ We hope that this series of theoretical studies will provide a useful guide for the interpretation of future CAD experiments on the $[\text{C}_2\text{H}_5\text{S}]^-$ anions.

2. Theoretical Method

All calculations were carried out using the Gaussian 94¹⁵ and Gaussian 98¹⁶ packages of programs. The computational method employed in this work is essentially the same as that used in our previous study on $[\text{C}_2\text{H}_5\text{O}]^-$ anions.¹³ The modified Gaussian-2 (G2++)¹³ procedure for ion–molecule reactions involving anions was used to obtain the energetics of the anionic species studied in this work. Structures were optimized at the MP2/6-31++G(d) level. All electrons were included in the calculation of electron correlation energies for all post-Hartree–

Fock (HF) optimizations and frequency calculations. The scaling factors 0.948 and 0.972 were used to scale the MP2/6-31++G(d) frequencies¹⁷ in the calculations of thermal corrections and zero-point energies (ZPE), respectively. All transition-state (TS) structures, except rotational TSs, were characterized by intrinsic reaction coordinate calculations.^{18,19} We used a factor of 0.95 for scaling^{20,21} the QCISD/6-31++G(d) or QCISD/6-31++G(d,p) frequencies in calculations of thermal corrections and ZPEs for species which were also optimized at these theoretical levels.

A stability test was carried out for all the zeroth-order, or HF reference, wave functions of all the optimized structures. Some of the $[\text{C}_2\text{H}_5\text{S}]^-$ isomers and TS structures with open-shell character had unstable restricted HF (RHF) functions; i.e., allowing the RHF determinant to become unrestricted (UHF) leads to a lower energy solution. Such problematic systems have been discussed previously.^{22,23} Molecular systems thought to be closed-shell species having RHF instability were also reoptimized at the UMP2/6-31++G(d) level with the optimized UHF reference wave functions as initial guess and subsequent single-point calculations for G2++ energies were carried out with the UHF formalism. In general, when the singlet is the true ground state for such a problematic system, its $G2_{\text{RQCISD}}$ energy (G2 energy calculated at the RQCISD/6-31G(d) optimized structure with the RHF formalism) is consistent with the $G2_{\text{UQCISD}}$ energy (G2 energy calculated at the UQCISD/6-31G(d) optimized structure with the UHF formalism).^{20,21}

A singlet ion–radical complex (IRCX) or an IRCX-like TS such as $[\text{S}^-\cdots\text{C}_2\text{H}_5]$ corresponds to an open-shell singlet. Hence, the use of a RHF reference wave function for the IRCX species implying both electrons with identical spatial distribution is not appropriate. Therefore, its structure was optimized at the UMP2/6-31++G(d) level with the optimized UHF function ($\langle S^2 \rangle \approx 1$) for the separated fragments as the initial guess. Such a method applied to an open-shell singlet has its limitations. The diradical-like state is poorly described by a single determinantal function. In addition, in the regions of the potential-energy surface (PES)

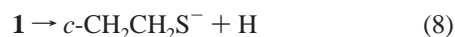
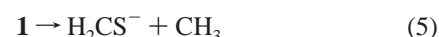
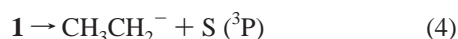
having a triplet ground state, energy calculations based on UHF formalism would give a poor approximation to the triplet energy.²⁴

For all IRCXs, $\langle S^2 \rangle$ is close to 1, as expected and desired. For all the TSs involving IRCX such as TS(**8**_{ircx}→**9**_{imc}), the values of $\langle S^2 \rangle$ range from 0.86 to 1.02. This type of TS is expected to have significant open-shell character. Other radicals such as H, H₂CS⁻, CH₃, etc. do not have serious spin contamination. Singlet species such as H₂CS and CH₃CHS have unstable RHF wave functions. Their optimized UHF wave functions have $\langle S^2 \rangle$ values of ca. 0.3. As will be seen in the results given in Table 1, as well as those in our previous work on the [C₂H₅S]⁺ systems,^{20,21} various energies calculated at the G2_{RMP2}, G2_{RQCISD}, and G2_{UQCISD} levels are consistent with each other, indicating that the degree of RHF instability associated with these species poses no serious effect in the accuracy of calculated energies.

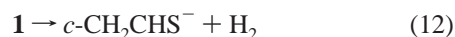
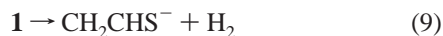
We denote G2_{UMP2}++ energies as G2++ energies calculated at UMP2/6-31++(d) optimized structures with the UHF formalism. Similarly, G2_{RMP2}++ denotes G2++ energies calculated at the RMP2/6-31++G(d) optimized structures with the RHF formalism. Unless stated otherwise, calculated energies and thermochemical properties discussed in this work refer to 0 K at the G2++ level (G2_{UMP2}++ for open-shell and G2_{RMP2}++ for closed-shell systems).

3. Results and Discussion

Conformers of CH₃CH₂S⁻ (**1**), CH₃CHSH⁻ (**2/3**), and CH₃SCH₂⁻ (**4/5**) are illustrated in Figure 1. Their calculated energies and thermochemical data, as well as those of other molecular species related in this work, are presented in Table 1. Table 2 lists the heats of reaction $\Delta H_{r,T}$ for various simple dissociations involving CH₃CH₂S⁻ (**1**):



Also listed in the same table are the $\Delta H_{r,T}$ and energy barriers ΔE_b for the following four elimination reactions of **1**:



The calculated $\Delta H_{f,298}$ values listed in Table 1 are in good agreement with the available experimental data,²⁵ except in the cases of H₂CS⁻ and CH₃CHS, which deviate from the calculated

values by more than 20 kJ mol⁻¹. This magnitude of deviation is well beyond the uncertainty (8.4 kJ mol⁻¹) of the G2 method.²⁶ Nevertheless, the G2++ $\Delta H_{f,298}$ value for H₂CS⁻ (82 kJ mol⁻¹) is in better agreement with the value (73 kJ mol⁻¹) derived from the observed electron affinity (0.465 ± 0.0023 eV)^{25,27} of H₂CS reported by Moran and Ellison and the $\Delta H_{f,298}$ value of H₂CS (118.0 ± 8.4 kJ mol⁻¹)^{25,28} reported by Ruscic and Berkowitz. The observed free energy change ($\Delta G_{r,298}$) for the reaction CH₃CHS → CH₂CHS⁻ + H⁺, i.e., the acidity of CH₃CHS, is 1427 kJ mol⁻¹.²⁵ Considering the experimental $\Delta H_{f,298}$ (145.2 kJ mol⁻¹) and entropy (108.96 J mol⁻¹ K⁻¹) values²⁵ for proton, the calculated acidity of CH₃CHS, 1422 kJ mol⁻¹, is in good agreement with the observed value. However, no experimental heat of formation for CH₂CHS⁻ is available.

Structures of ion–neutral complexes (INCs), which include both IMCs and IRCXs, and TSs involved in reactions 9, 10, 11, and 12 are shown in Figures 2a, 3a, 4a, and 5a, respectively. Their corresponding G2++ PESs are illustrated in Figures 2b, 3b, 4b, and 5b, respectively.

3.1. Thioethoxyl Anion (1). Thioethoxyl anion (**1**) is the most stable isomer found on the hypersurface of the [C₂H₅S]⁻ anions studied in this work. Its calculated heat of formation ($\Delta H_{f,298}$) is -86 kJ mol⁻¹, in good agreement with the experimental value (-90.4 ± 9.6 kJ mol⁻¹).²⁵ The rotational TS **1a** is 14 kJ mol⁻¹ above **1**. Using the G2_{UMP2} $\Delta H_{f,0}$ value (115 kJ mol⁻¹)²⁹ of CH₃CH₂S, we obtained an electron affinity (EA) value of 1.94 eV for the radical, consistent with the experimental values which span the range from 1.947 to 1.97 eV.^{25,30,31} The EAs of alkoxy and thioalkoxy radicals follow the trend EA(R'X) > EA(RX), where R' is a larger alkyl group than R and X is O or S.³¹ Using the perturbative molecular orbital model,^{32–34} Janousek et al.³¹ rationalized the EA trend of RX: a larger R has a larger stabilizing effect on RX⁻ due to more alkyl π^* orbitals available for the stabilizing interactions with the nonbonding (lone-pair) orbitals on X, but the stabilizing effect of R on RX is far less than that on RX⁻.

It is interesting to compare the structural changes of RX on conversion to RX⁻. The extent of these changes may reflect the relative strength of stabilizing effects of R on RX⁻. In RX⁻, the orbital interaction between the nonbonding orbitals on X, n(X), and the alkyl $\pi^*(R)$ orbitals is stabilizing and has the effects of lengthening the C_β-H (CH₂-H) bonds^{29,31} and delocalizing the negative charge on X into the R group. The two-orbital-four-electron interaction n(X)- $\pi(R)$ is repulsive (destabilizing) and has the effects of weakening the C-X bond²⁹ and localizing the negative charge on X. For CH₃CH₂X⁻, the stabilizing interaction n_a(X)- $\pi^*_a(R)$ results in lengthening the $\sigma(C-C)$ bond. As a consequence of these stabilizing interactions, the negative charge on the X atom delocalizes onto the R group, and the C-X bond is shortened due to the net π bonding between the X and C_β atoms.

On conversion from RO to RO⁻, the C-O bond length decreases by ca. 0.03–0.04 Å, and the C_β-H bond length increases by ca. 0.03 Å (Table 3). In addition, the C-C bond length of the anion is longer than that of the neutral by 0.03 Å. All these changes indicate that the stabilizing interactions are dominant in RO⁻. On the other hand, the C-S bond length (1.82–1.83 Å) of RS⁻ is ca. 0.02–0.03 Å longer than that of RS (1.80 Å). The C_β-H and C-C bond lengths increase very slightly by less than 0.01 Å from RS to RS⁻. These results lend support to the postulation that there is a competing alkyl group destabilizing effect in RS⁻ in addition to the stabilizing

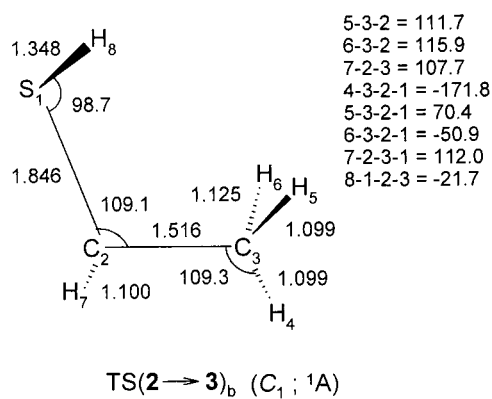
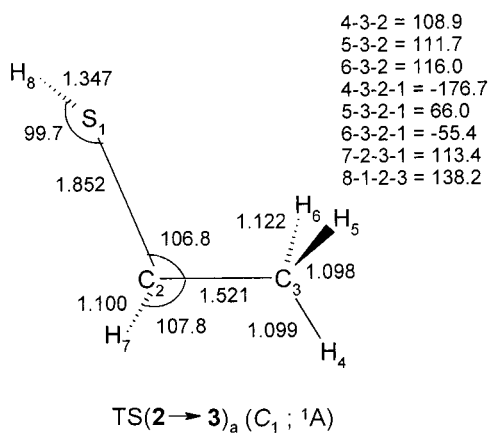
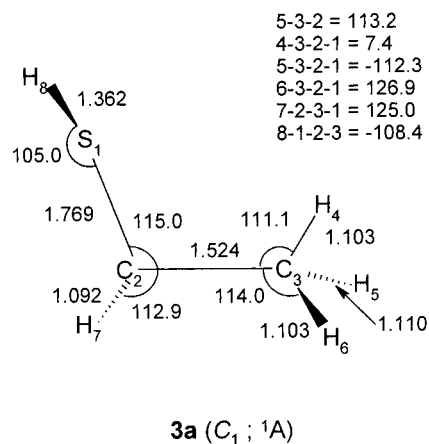
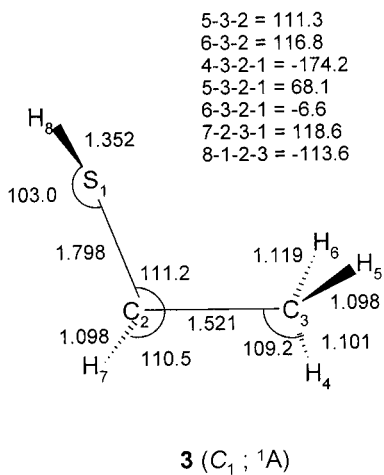
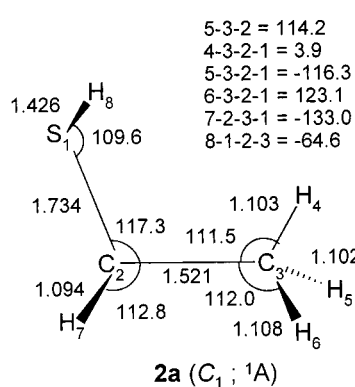
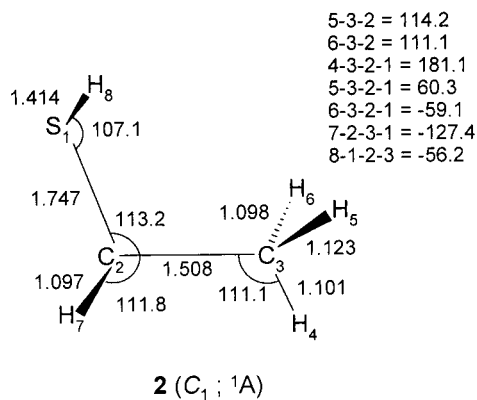
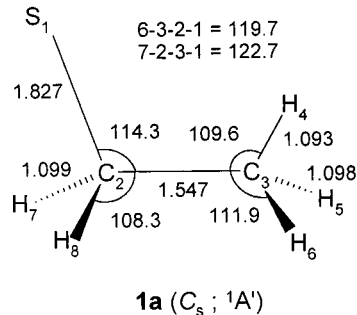
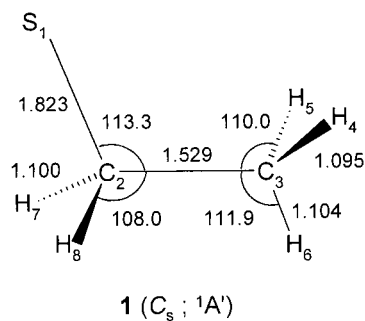
TABLE 1: G2++ Electronic Energies E_e (hartrees), Scaled Zero-Point Energies ZPE (mhartrees), and Enthalpies of Formation $\Delta H_{f,T}$ (kJ mol⁻¹) at 0 and 298 K for [C₂H₅S⁺] Systems and Other Molecular Species Related in This Work

species	E_e	ZPE	$\Delta H_{f,0}$		$\Delta H_{f,298}$		method ^a
			G2	G2	experiment ^b		
1	-476.87456	64.72	-72.5	-85.9		-90.4 ± 9.6	
2	-476.80671	58.75	89.9	77.5			
3	-476.80034	59.39	108.3	96.5			
4	-476.80576	60.48	97.0	85.8		77.4 ± 9.2 ^c	
5	-476.80645	59.77	93.3	82.5			
6_{imc}	-476.76604	54.81	186.4	177.4			
7_{imc}	-476.83761	53.30	-5.5	-13.0			
8_{irrx}	-476.76897	59.88	192.0	184.0			
	-476.76899	58.37	187.9	180.0			G2UQCISD++ ^d
9_{imc}	-476.85202	57.26	-32.9	-39.5			
10_{imc}	-476.75601	54.30	211.3	206.6			
11_{irrx}	-476.75610	53.64	209.4	206.0			
12_{imc}	-476.79333	56.66	119.6	114.9			
13_{imc}	-476.75800	55.84	210.2	200.8			
14_{imc}	-476.75950	56.26	207.3	196.7			
15_{imc}	-476.76027	53.38	197.7	189.1			
1a	-476.86871	64.15	-58.7	-73.3			
2a	-476.80094	57.98	103.1	89.5			
3a	-476.79633	58.75	117.2	103.9			
4a	-476.80327	60.62	103.9	90.7			
5a	-476.80416	59.50	98.6	86.0			
TS(1→3)	-476.76813	56.84	186.2	173.9			
TS(1→6 _{imc})	-476.76678	54.48	183.5	172.6			
TS(1→8 _{irrx})	-476.76815	60.4	194.8	184.6			
TS(1→11 _{irrx})	-476.75992	54.28	201.0	194.3			
TS(1→12 _{imc})	-476.75647	53.01	206.8	197.4			
	-476.75576	53.01	208.6	199.3			G2RQCISD++
	-476.75905	56.25	208.5	195.7			
TS(2→3) _a	-476.79029	58.72	132.9	119.9			
TS(2→3) _b	-476.79145	58.86	130.3	117.0			
TS(2→3) _i	-476.79663	57.42	112.9	100.4			
TS(4→5)	-476.78903	60.25	140.3	127.4			
TS(4→5) _i	-476.80522	59.32	95.4	83.5			
TS(6 _{imc} →7 _{imc})	-476.76513	54.4	187.7	176.7			
TS(8 _{irrx} →9 _{imc})	-476.77538	55.46	163.5	152.2			
	-476.77086	54.37	172.6	161.1			G2UQCISD++ ^d
TS(11 _{irrx} →12 _{imc})	-476.75122	53.17	220.9	211.7			
	-476.75203	53.17	218.8	209.6			G2UQCISD++
TS(13 _{imc} →14 _{imc})	-476.75793	55.74	210.1	198.4			
TS(14 _{imc} →14 _{imc})	-476.75892	55.88	207.9	195.6			
TS(14 _{imc} →15 _{imc})	-476.74597	51.57	230.5	218.5			
H	-0.5		216.035 ^{e,f}	217.998 ^{e,f}		217.998 ± 0.006	
H ⁻	-0.52270		156.4	158.4		145.2	
C (triplet)	-37.78449		711.194 ^e	716.68 ^{e,f}		716.68 ± 0.45	
						716.669	
						277.17 ± 0.15	
S (triplet)	-397.65534		274.925 ^{e,f}	277.17 ^{e,f}		276.9804	
						76.78	
S ⁻	-397.72917		81.1	83.4		-81.2 ± 9.2	
HS ⁻	-398.37824	5.92	-78.7	-78.2		-68.62	
HCS ⁻	-436.33355	10.86	197.0	198.2			
H ₂ CS	-436.95767	23.70	119.4	116.4		118.0 ± 8.4	G2RMP2
	-436.95766	23.93	120.0	117.1		90.0 ± 8.0	G2RQCISD
	-436.95681	24.05	122.5	119.1			G2UQCISD
H ₂ CS ⁻	-436.97032	22.23	83.9	82.1		73 ^g	
						55.6 ± 13.0	
<i>anti</i> -HSCH ₂ ⁻	-437.54899	31.56	117.7	111.9			
<i>syn</i> -HSCH ₂ ⁻	-437.55140	30.82	109.4	103.4			
	-436.95681	24.05	122.5	119.6			
CH ₃	-39.77274	28.40	151.5	148.9		145.6873	G2UMP2
						147.0 ± 1.0	
CH ₃ ⁻	-39.77573	28.78	145.1	141.9		138.5 ± 3.8	
CH ₄	-40.45355	43.13	-68.5	-76.1		-74.8731	G2RMP2
CH ₃ CH ₂	-79.02673	57.18	137.2	127.5		119.0 ± 2.0	G2UMP
CH ₃ CH ₂ ⁻	-79.02073	57.83	155.6	144.8		144.0 ± 8.8	
CH ₃ CHS	-476.21980	51.43	80.9	71.8		50.0 ± 8.0	G2RMP2
	-476.21979	52.00	82.4	73.3			G2RQCISD
	-476.21887	52.13	85.2	76.0			G2UQCISD
CH ₃ CHS ⁻	-476.22718	51.01	62.4	53.9			
CH ₂ CHS ⁻	-475.65802	40.35	-0.1	-5.9			
<i>c</i> -CH ₂ CHS ⁻	-475.57944	40.27	206.0	199.5			
<i>c</i> -CH ₂ CH ₂ S	-476.21977	55.12	92.6	81.7			
C ₂ H ₄	-78.46484	48.43	60.7	53.0		52.46694	G2RMP2

^a G2++, unless otherwise stated explicitly. ^b Data from ref 25, unless otherwise stated explicitly. ^c The experimental value does not distinguish between **4** and **5**. ^d Based on UQCISD/6-31++G(d,p) structure. ^e Ref 71. ^f Experimental $\Delta H_{f,T}$ values used as G2++ $\Delta H_{f,T}$ values for elements in G2++ parametrization. ^g Calculated by using the experimental EA(H₂CS)²⁷ = 0.465 eV and $\Delta H_{f,298}$ (H₂CS)²⁸ = 118.0 kJ mol⁻¹.

interaction $n(X)-\pi^*(R)$.³¹ It appears that the overall stabilizing effect of R on RX⁻ is relatively weaker in RS⁻ than in RO⁻. As a consequence of the dominant destabilizing interaction $n(S)-\pi(R)$, the S atom of RS⁻ is more negatively charged than the O atom of CH₃CH₂O⁻ (Table 3).

3.2. α -SR (R = H, CH₃) substituted carbanions CH₃CHSH⁻ (2/3) and CH₃SCH₂⁻ (4/5). Both 1-mercaptoethyl anion (**2**, **3**) and methylthiomethyl anion (**4**, **5**) have two possible conformations, the syn form (**2**, **5**) and the anti form (**3**, **4**). Like the parent mercaptomethyl anion HSCH₂⁻,³⁵ the syn conformation



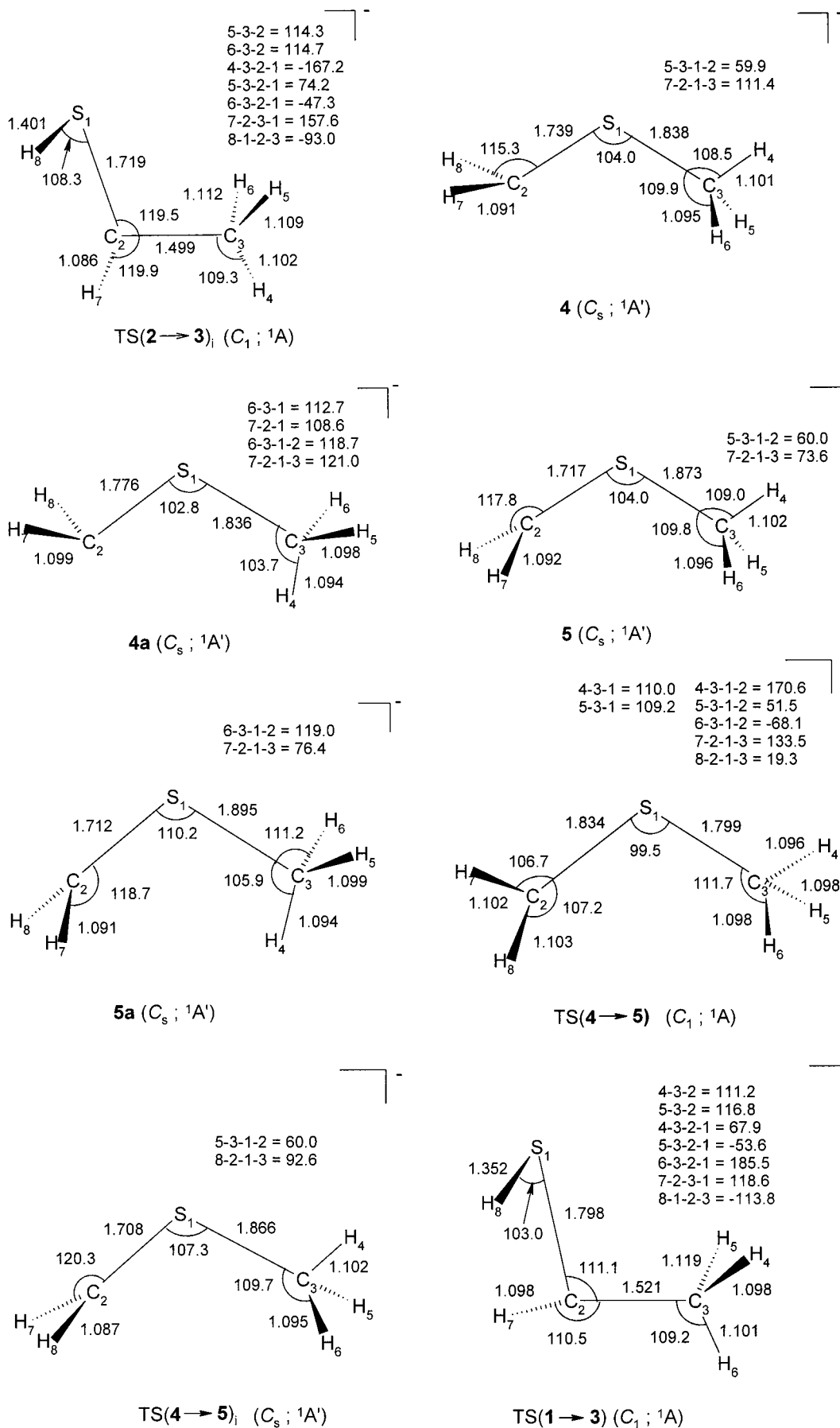


Figure 1. MP2/6-31++G(d) optimized structures of [C₂H₅S]⁻. is favored for these α -SR substituted carbanions. For HSCH₂⁻, the syn conformer has lower energy than the anti-conformer

by 8 kJ mol⁻¹, and the rotational barrier for *syn*-HSCH₂⁻ → *anti*-HSCH₂⁻ is 38 kJ mol⁻¹ at the G2++ level.

TABLE 2: Heats of Reaction $\Delta H_{r,T}$ (kJ mol⁻¹) for Simple Dissociations and Elimination Reactions of CH₃CH₂S⁻(1**) and Energy Barriers ΔE_b (kJ mol⁻¹) for the Elimination Reactions of **1****

reaction	$\Delta H_{r,0}$		$\Delta H_{r,298}$		ΔE_b
	G2++	G2++	experiment ^a		
(1) 1 → CH ₃ CHS + H ⁻	310.2	316.1	285.6		
(2) 1 → CH ₃ CHS ⁻ + H	350.9	357.8			
(3) 1 → CH ₃ CH ₂ + S ⁻	290.8	297.6	286.2		
(4) 1 → CH ₃ CH ₂ ⁻ + S (triplet)	503.0	508.0	511.4		
(5) 1 → H ₂ CS ⁻ + CH ₃	307.8	313.9	291.7, 293.0		
(6) 1 → H ₂ CS + CH ₃ ⁻	337.0	344.2	346.9		
(7) 1 → <i>c</i> -CH ₂ CH ₂ S + H ⁻	321.5	325.9			
(8) 1 → <i>c</i> -CH ₂ CH ₂ S ⁻ + H	465.9	470.4			
(9) 1 → CH ₂ CHS ⁻ + H ₂	68.1	77.1			260.0
(10) 1 → CH ₂ CH ₂ + HS ⁻	55.5	60.7	61.7, 74.3		267.0
(11) 1 → CH ₄ + HCS ⁻	201.0	208.0			293.0
(12) 1 → <i>c</i> -CH ₂ CHS ⁻ + H ₂	245.6	249.5			303.0

^a Calculated from observed $\Delta H_{f,298}$ values for individual molecular species as listed in Table 1.

TABLE 3: Some Structural Properties of RX (R = Me, Et and X = O, S) and RX⁻

	MeO/EtO	MeO ⁻ /EtO ⁻	MeS/EtS	MeS ⁻ /EtS ⁻
C-X (Å)	1.389/1.392	1.356/1.353	1.798/1.803	1.831/1.823
C-C (Å)	-/1.518	-/1.548	-/1.522	-/1.529
C _β -H ^a (Å)	1.097/1.102	1.131/1.131	1.093/1.097	1.099/1.100
charge on X atom (<i>e</i>)	-0.242/-0.227	-0.868/-0.802	0.036/0.032	-0.906/-0.868

The calculated $\Delta H_{f,298}$ values for **2** and **3** are 78 and 97 kJ mol⁻¹, respectively. The rotational TSs **2a** and **3a** lie 13 and 9 kJ mol⁻¹ above **2** and **3**, respectively. Conformational change **2** → **3** may proceed through rotation about the C_α-S bond or inversion at the anionic center. The rotational TSs TS(**2**→**3**)_a and TS(**2**→**3**)_b are 40 and 43 kJ mol⁻¹, respectively, above **2**. Inversion occurs via TS(**2**→**3**)_i, which is 23 kJ mol⁻¹ higher in energy than **2** and is the lowest-energy process that leads to a conformational change of **2**.

The anti (**4**) and syn (**5**) conformers of the methylthiomethyl anion have similar energies. The calculated $\Delta H_{f,298}$ values for **4** and **5** are 86 and 83 kJ mol⁻¹, respectively, in good agreement with the experimental value,²⁵ 77.4 ± 9.2 kJ mol⁻¹. The methyl group of **4/5** rotates about the CH₃-S bond with a small barrier. The rotational TSs **4a** and **5a** are 7 and 5 kJ mol⁻¹ higher in energy than **4** and **5**, respectively. On the other hand, the barrier to rotation about the C_α-S (CH₂-S) bond of **5** is rather high, 47 kJ mol⁻¹. The high rotational barriers to the corresponding C_α-S bonds of HSCH₂⁻, CH₃CHSH⁻, and CH₃SCH₂⁻ will be discussed later in this section. The rotational TS(**4**→**5**) has C₁ symmetry. The inversion TS(**4**→**5**)_i is 2 kJ mol⁻¹ above **5** and below **4**, respectively. The anomaly that a TS is slightly lower in energy than a local minimum to which it connects has been discussed previously.³⁶ Similar values for these rotational and inversion barriers have been calculated by Wiberg and Castejon.³⁷

It is worthwhile to note that the S-R (R = H for **2/3**, CH₃ for **4/5**) bonds of the syn conformers of the α-SR substituted thiocarbanions are substantially longer than those of the corresponding anti conformers. The S-H bond of **2** (1.414 Å), which is approximately antiparallel to the anionic lone-pair orbital, n(C_α), is substantially longer than that (1.352 Å) of **3**. At the same time, the C_α-S bond length (1.747 Å) of the former is significantly shorter than that (1.798 Å) of the latter. This pattern of structural features is also found in the syn and anti conformers of HSCH₂⁻.³⁵ In addition, the C_β-H bond antiparallel to the anionic lone pair n(C_α) is the longest (1.12 Å) among

TABLE 4: Stabilization Energies (kJ mol⁻¹) for Orbital Interactions n(C_α)-σ*(S-R) and n(C_α)-σ*(C_β-H)^a

orbital interaction	stabilization energy					
	<i>syn</i> -HSCH ₂ ⁻	<i>anti</i> -HSCH ₂ ⁻	2 (<i>syn</i>)	3 (<i>anti</i>)	5 (<i>syn</i>)	4 (<i>anti</i>)
n(C _α)-σ*(S-H)	82	39	77	30	92	53
n(C _α)-σ*(C _β -H)			50	52		

^a Here R = H for HSCH₂⁻ and **2/3**, and R = CH₃ for **4/5**. The σ(C_β-H) bond is approximately antiparallel to the anionic lone pair n(C_α).

the C-H bonds of the CH₃CHS⁻ conformers. Similarly, **5** has a shorter C_α-S bond length (1.717 Å) than **4** (1.739 Å). However, the C_γ-S (CH₃-S) bond of **5** is ca. 0.03 Å longer than that (1.838 Å) of **4**.

The preferred syn conformation of HSCH₂⁻ was proposed^{38,39} to arise from negative hyperconjugation⁴⁰ involving delocalizing the anionic lone pair n(C_α) into a low-lying σ*(S-H) antibonding orbital. The interaction can be studied with the natural bond orbital (NBO) formalism of Reed and Weinhold et al.⁴¹ The stabilization energy due to the orbital interaction n(C_α)-σ*(S-H), for example, can be evaluated by the following steps: (i) zero the off diagonal NBO Fock matrix element between n(C_α) and σ*(S-H) or delete the antibonding orbital σ*(S-H); (ii) the altered NBO Fock matrix is then subjected to one SCF cycle; (iii) calculate the difference between the SCF energies of the altered and unaltered NBO matrices. Using the NBO routine implemented in the Gaussian98 package of programs, we calculated the stabilization energies for the orbital interactions n(C_α)-σ*(S-R) and n(C_α)-σ*(C_β-H) for the α-SR substituted carbanions. They are listed in Table 4, from which one can see that the orbital interaction n(C_α)-σ*(S-R) is relatively stronger in the syn conformers of the thiocarbanions than the corresponding anti conformers. For **2** and **3**, the anionic lone pair also has significant interaction with the σ*(C_β-H) orbital which is approximately antiparallel to the n(C_α) orbital. These orbital interactions tend to weaken (or lengthen) the S-R and C_β-H bonds. The orbital interaction n(C_α)-σ*(S-R) also has a net π-bonding effect between the C_α and S atoms.^{39,42} The large barriers (38–47 kJ mol⁻¹) to rotation about the C_α-S bonds of HSCH₂⁻, CH₃CHSH⁻, and CH₃SCH₂⁻ suggest that they have significant double-bond character. This is in accord with the calculated bond order value (1.4)³⁶ for **5**. The lengthening and shortening of the S-R and C_α-S bonds, respectively, in the syn conformers of HSCH₂⁻, CH₃CHSH⁻, and CH₃SCH₂⁻ as compared to the corresponding anti conformers are consistent with the hypothesis of negative hyperconjugation.

It has also been proposed⁴² that the preferential stabilization of the thiocarbanions versus the corresponding oxy analogues is controlled by the inductive effect of the C-X (X = O, S) bond rather than the negative hyperconjugation. Although the latter model accounts well for the structural features of the conformers of α-SR substituted carbanions and the observed stereochemistry of carbanion formation adjacent to sulfur,⁴³ it has been pointed out⁴⁴ that the high polarizability of sulfur must be invoked to account for the large stabilization of the mercaptomethyl anion.

3.3. β-SH Substituted Carbanion HSCH₂CH₂⁻. Unlike the corresponding oxygen analogue,¹³ the 2-mercaptoethyl anion (HSCH₂CH₂⁻) is unstable with respect to dissociation to HS⁻ + ethylene (C₂H₄) without an energy barrier. This corresponds to complete charge transfer to the HS fragment. Optimizations starting from the structures of 2-mercaptoethyl radical²⁹ HSCH₂-CH₂ and various conformations of the frozen thiocarbanion,

obtained by removing a proton from the methyl group of the optimized CH₃CH₂SH structures, lead to an IMC structure, [C₂H₄...HS]⁻. Previous theoretical studies^{45,46} show that β-fluoroethyl anion, whose valence shell is isoelectronic with HSCH₂CH₂⁻, is unstable with respect to dissociation to F⁻ + C₂H₄ without an energy barrier.

In the review article of Nobes et al.,⁴⁷ it is stated that ethyl anions XCH₂CH₂⁻ with electronegative β substituents (X = F, PH₂, SH, and Cl) are generally unstable with respect to elimination and there is essentially complete transfer of the negative charge from the anionic center to X, resulting the formation of a complex of ethylene with X⁻. However, HOCH₂CH₂⁻ is a local minimum.^{13,47} It is interesting to note that the electron affinities (EA) of F (3.4 eV),²⁵ SH (2.3 eV),²⁵ and Cl (3.6 eV)²⁵ are all larger than that of OH (1.8 eV),²⁵ except the EA of PH₂ (0.96–1.6 eV).²⁵ On the basis of this observation, one may postulate that XCH₂CH₂⁻ is unstable with respect to dissociation to C₂H₄ + X⁻ without an energy barrier for EA(X) > EA(OH) and XCH₂CH₂⁻ corresponds to a local minimum when EA(X) ≤ EA(OH). The anomaly that PH₂ has EA value < EA(OH) and H₂PCH₂CH₂⁻ does not correspond⁴⁷ to a local minimum found in previous studies prompted us to repeat the optimization studies of XCH₂CH₂⁻ at the MP2/6-31++G(d) level. We found a local minimum that corresponds to H₂PCH₂CH₂⁻ on the MP2/6-31++G(d) PES, and no local minimum corresponding to XCH₂CH₂⁻ was identified for X = F, SH, and Cl.

3.4. Direct Dissociations of CH₃CH₂S⁻ (1). Intuitively, one would expect that the occurrence of homolytic cleavage AB⁻ → A + B⁻ or heterolytic dissociation AB⁻ → A⁻ + B to be controlled by simple thermochemical considerations so that product stability should be a determining factor, provided that both channels have no reverse barrier. Thus, heterolytic C_β-H (CH₂-H) bond fission (reaction 1) occurs more likely than homolytic C_β-H bond cleavage (reaction 2). The C-S bond cleavage of **1** (reaction 3) is exclusively homolytic because of the large ΔH_{r,0}(4) value. Homolytic C-C bond cleavage of **1** (reaction 5) is energetically more competitive than heterolytic cleavage of the C-C bond (reaction 6). Heterolysis of the C_γ-H (CH₃-H) bond (reaction 7) leads to the formation of thiirane (c-CH₂CH₂S). Among these simple bond fissions, reaction 3 is the most energetically probable. From an energetic viewpoint, the C-C and C-S bond cleavages are homolytic while the C-H bond fissions are heterolytic.

3.5. Elimination Reactions of 1. Reactions 9 and 10 are 1,2-elimination reactions, while reactions 11 and 12 proceed via 1,1-elimination pathways. Reaction 12 may also proceed via a 1,2-elimination pathway which has the same energy barrier as that of the 1,1-elimination pathway. This will be discussed in section 3.5.4.

In general, a 1,2-elimination reaction is highly asynchronous and is INC-mediated.^{10,48–52} In the unimolecular decomposition of a variety of gaseous ions, INCs or INC-like complexes are formed^{12,53,54} via a dissociative mechanism.⁵⁵ In this mechanism, a covalent bond cleaves in such a fashion that the charged and neutral fragments are held together by electrostatic interaction and the fragments sojourn in the vicinity of one another long enough to undergo a subsequent ion-neutral reaction.^{53,56} Such an INC may not necessarily correspond to a local potential energy minimum.⁵⁶ The internal rotational degrees of freedom developed within the complex provide an entropy well in which the system tends to linger.¹² The PES of this entropy well environ should be rather flat so that the lingering fragments can freely rotate relative to each other. The entropy bottleneck

may^{57–59} or may not^{60,61} be able to control the rate of dissociation. It is generally accepted that a species will be considered as an INC only if its lifetime from the point of covalent bond breaking to the point of overcoming long-range electrostatic forces is long enough that a chemical reaction other than dissociation has time to occur. Reactions mediated by INCs are generally stepwise from entropy consideration.^{12,53,54,56} Terms such as “INC” and “INC-like TS” invoked throughout this paper merely stress that the complex described corresponds to a local minimum or a saddle point on the MP2/6-31++G(d) PES.

Since the fragments of an INC [A...B]⁻ show reactivities similar to those expected for the isolated species,⁵⁴ it is not unreasonable to expect that it is dominated by either the [A⁻...B] or [A...B⁻] state. One may therefore infer the nature of INC-mediated reactions by comparing the energetics of the two limiting (heterolytic and homolytic) pathways. The stabilization energy of an INC relative to its separated fragments with a nonpolar neutral is ca. 20–25 kJ mol⁻¹.⁶² Stabilization energies in the range of 42–80 kJ mol⁻¹ are common in INCs containing a polar neutral.^{54,63} The energy barriers for the two limiting pathways can then be easily estimated from the stabilization energies of the INCs formed and the ΔH_{r,0} values for the homolytic and heterolytic dissociations.

3.5.1. 1,2-H₂ Elimination of 1 (Reaction 9). By comparing the ΔH_{r,0} values for reactions 1 and 2, the stabilization energies of [H...CH₃CHS⁻] and [H⁻...CH₃CHS] due to ion-dipole interaction, and assuming the elimination reaction is INC-mediated, one can infer that reaction 9 occurs by a heterolytic pathway. On the MP2/6-31++G(d) PES, heterolytic cleavage of the CH₂-H bond of **1** leads to the formation of **6_{imc}** via TS(**1**→**6_{imc}**). Subsequent proton transfer within **6_{imc}** yields **7_{imc}** via TS(**6_{imc}**→**7_{imc}**). Structures of TS(**1**→**6_{imc}**), **6_{imc}**, **7_{imc}**, and TS(**6_{imc}**→**7_{imc}**) are shown in Figure 2a. The IMC **7_{imc}** is formed from the final product pair prior to dissociation. When considering the possible intermediacy of INCs in unimolecular dissociations, a distinction must be made between processes in which the incipient product pair forms a stable complex prior to dissociation, and processes involving INCs as intermediates before the last chemical step.⁶⁴

As shown in Figure 2b, the G2++ energies of **6_{imc}**, TS(**1**→**6_{imc}**) and TS(**6_{imc}**→**7_{imc}**) are very close. Reaction 9 thus essentially has an energy barrier of 260 kJ mol⁻¹ over which a wide spectrum of INC-like structures exists. The [H⁻...CH₃CHS] complex has a finite lifetime because of the entropy effects due to the internal rotational degrees of freedom developed within the complex and is entropy stable. Proton transfer within the complex leading to **7_{imc}** is possible when the lingering fragments align in a proper relative orientation. In addition, the developed internal rotations (whose axes are perpendicular to the inter-fragment axis) have to transform into bending motions before a H-bridge can form between the fragments.⁵³ All these have an entropy cost and may take the form of an entropy barrier to the proton-transfer step.⁵³ In contrast to the TS for the proton-transfer step in the loss of H₂ from CH₃CH₂O⁻, which has a H-bridged structure [OCHCH₂...H...H]⁻,¹³ TS(**1**→**6_{imc}**) is very IMC-like. This suggests that the primary isotopic effect for the proton-transfer step would be very small. A large primary isotope effect for this step would require a significant lengthening the bridging C-H bond in the TS structure. This proton transfer process would proceed through a highly asymmetric TS (in term of the proton-bridged structure [C...H...H]⁻) due to the large exothermicity (ca. 192 kJ mol⁻¹) of this step and therefore should exhibit a small primary isotope effect.⁶⁵

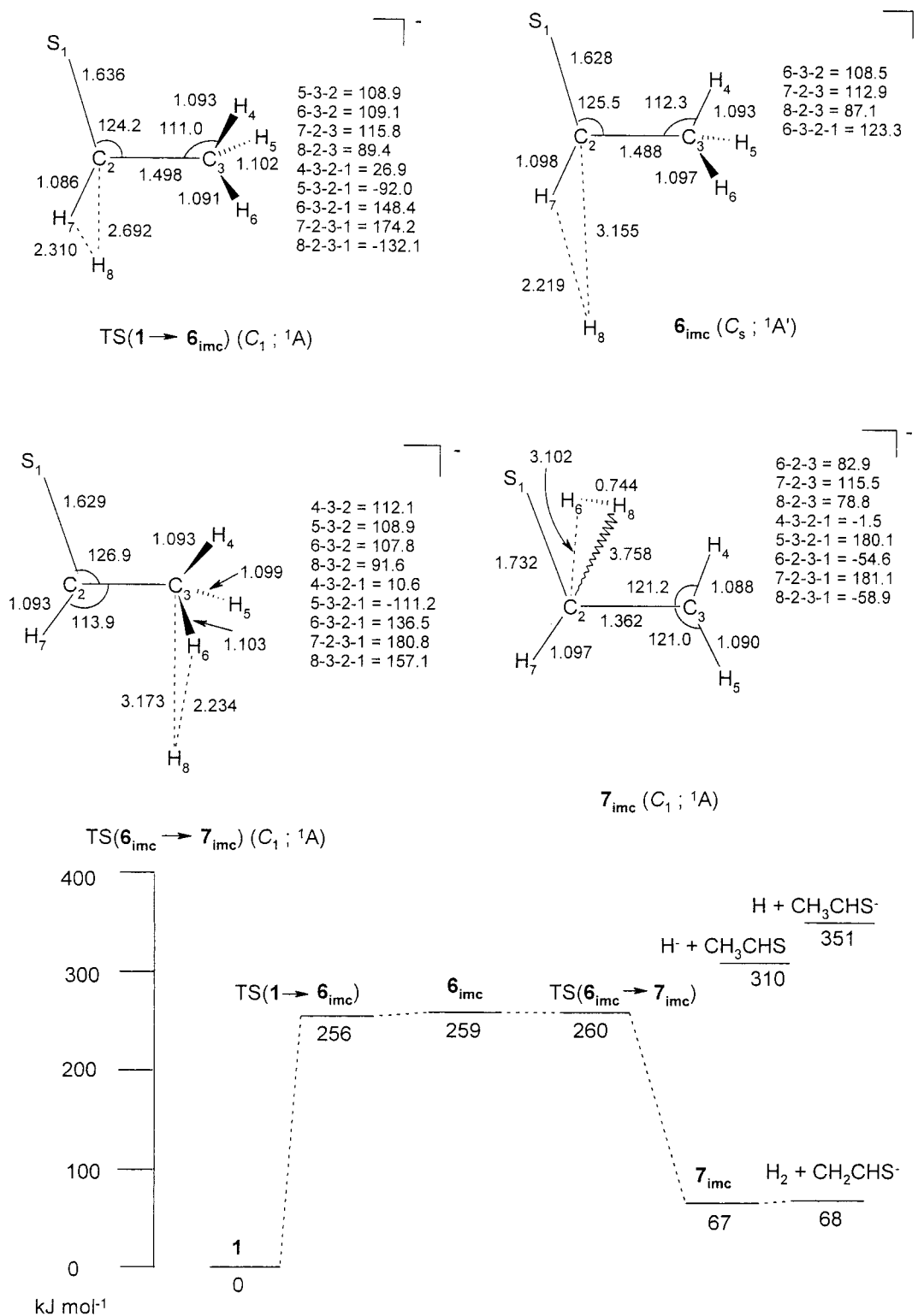
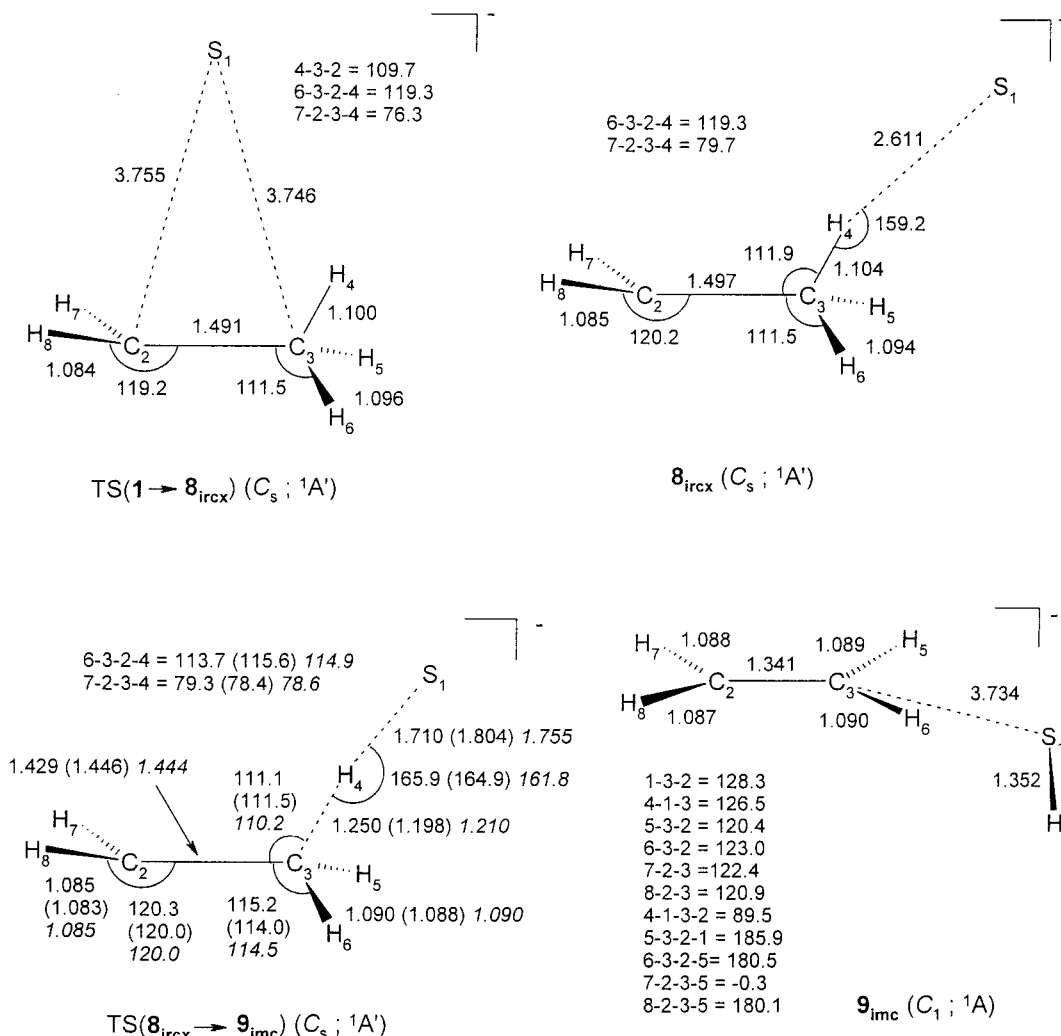


Figure 2. (a) MP2/6-31++G(d) optimized INC and TS structures for reaction 9. (b) Potential energy surface for reaction 9.

The overall energy barrier to $\text{CH}_3\text{CH}_2\text{O}^- \rightarrow \text{H}_2 + \text{CH}_2\text{CHO}^-$ is 126 kJ mol^{-1} .¹³ Thus, reaction 9 is a high-energy process as compared to the 1,2-elimination of H_2 from the oxygen analogue of **1**.

3.5.2. 1,2-HS⁻ Elimination of I⁻ (Reaction 10). Consideration of the $\Delta H_{r,0}$ values for reactions 3 and 4 leads to an intuitive conclusion that reaction 10 would take place via a homolytic mechanism if it is INC-mediated. On the UMP2/6-31++G(d) PES, reaction 10 proceeds as follows: **1** → TS(**1** → **8_{irxc}**) → **8_{irxc}** → TS(**8_{irxc}** → **9_{imc}**) → **9_{imc}** → $\text{C}_2\text{H}_4 + \text{HS}^-$. The $G2_{\text{UMP}2++}$

energies of the IRCX-like structures **8_{irxc}**, and TS(**1** → **8_{irxc}**) are essentially the same those as shown in Figure 3b. However, TS(**8_{irxc}** → **9_{imc}**) which shows some H-bridged character is ca. 29 kJ mol^{-1} lower in energy than **8_{irxc}**. This magnitude of deviation is certainly beyond the previously discussed anomaly that a TS is slightly lower in energy than a local minimum to which it connects.³⁶ A search for the TS was also repeated at both the UMP2/6-311++G(d,p) and UQCISD/6-31++G(d,p) levels. Both the UMP2/6-311++G(d,p) and UQCISD/6-31++G(d,p) structures (Figure 3a) of TS(**8_{irxc}** → **9_{imc}**) are quite similar and



UQCISD/6-31++G(d,p) structural parameters: Numbers in parentheses.
 UMP2/6-311++G(d,p) structural parameters: *Italic numbers*.

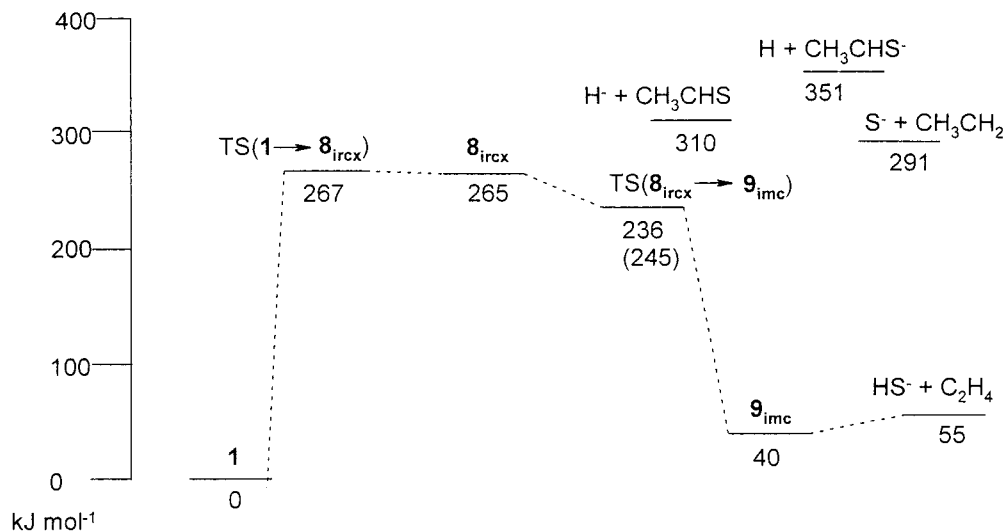


Figure 3. (a) MP2/6-31++G(d) optimized INC and TS structures for reaction 10. (b) Potential energy surface for reaction 10.

have a shorter bridging C–H bond (1.2 Å) and longer H...S distance (1.75–1.80 Å) than the UMP2/6-31++G(d) structure. Repeated IRC calculations for TS($\mathbf{8}_{ircx} \rightarrow \mathbf{9}_{imc}$) at the UMP2/6-311++G(d,p) level yield the same conclusion: TS($\mathbf{8}_{ircx} \rightarrow \mathbf{9}_{imc}$) connects $\mathbf{8}_{ircx}$ and $\mathbf{9}_{imc}$. The G2_{UQCISD}++ results based on the UQCISD/6-31++G(d,p) structures of $\mathbf{8}_{ircx}$ and TS($\mathbf{8}_{ircx} \rightarrow \mathbf{9}_{imc}$)

indicate that the former is still 15 kJ mol⁻¹ higher in energy than the latter. With no ZPE correction included in their G2_{UQCISD}++ energies, $\mathbf{8}_{ircx}$ is ca. 5 kJ mol⁻¹ above TS($\mathbf{8}_{ircx} \rightarrow \mathbf{9}_{imc}$). Thus, TS($\mathbf{8}_{ircx} \rightarrow \mathbf{9}_{imc}$) does not correspond to a local stationary point on the G2++ PES. Discrepancy between results of lower (e.g., HF) and higher (e.g., MP2) theoretical methods

for nonclassical structures as in the cases of ethyl cation⁶⁶ and C–C protonated oxirane²² is not uncommon. In addition, molecular species which have extensive open-shell character such as TS(**8**_{ircx}→**9**_{imc}) may suffer from certain unsatisfactory features of the convergence behavior of UMPn energies.^{67,68}

In summary, reaction 10 has an energy barrier of 267 kJ mol⁻¹ and proceeds via a homolytic C–S bond cleavage to form the [S⁻...CH₃CH₂] complex (TS(**1**→**8**_{ircx})), followed by H transfer within the complex. The landscape of this PES is similar to that for reaction 9. Reactions 9 and 10 are energetically competitive.

3.5.3. 1,1-CH₄ Elimination of 1 (Reaction 11). One may expect that reaction 11 is also INC-mediated, similar to the corresponding reaction for the oxygen analogue of **1**, which has been studied at the same theoretical level.¹³ A complex [CH₃⁻...H₂CS] as illustrated by **10**_{imc} was identified. It is ca. 53 kJ mol⁻¹ lower in energy than CH₃⁻ + H₂CS. Complex [CH₃⁻...H₂CS⁻] such as **11**_{ircx} is ca. 26 kJ mol⁻¹ lower in energy than CH₃ + H₂CS⁻. The Δ*H*_{f,0} values for **10**_{imc} and **11**_{ircx} are 211 and 209 kJ mol⁻¹, respectively. From the Δ*H*_{r,0} values for reactions 5 and 6 (Table 2) as well as the stabilization energy (20–25 kJ mol⁻¹ for a nonpolar fragment⁶² and 42–80 kJ mol⁻¹ for a polar fragment^{54,63}) of an INC relative to its separated fragments, one arrives at the same conclusion that **10**_{imc} and **11**_{ircx} are similar in energy. Then, is reaction 11 IRCX-mediated or IMC-mediated?

At the RMP2/6-31++G(d) level, TS(**1**→**12**_{imc}), which connects **1** and **12**_{imc} ([CH₄...HCS⁻]) and has a H-bridged structure, was identified. Certainly, TS(**1**→**12**_{imc}) and its nearby environs have extensive open-shell character, and their corresponding RHF functions are likely to have RHF instability. The validity of RMPn energies based on unstable RHF functions has been questioned.⁶⁹ The energy barrier to this heterolytic pathway, as implicitly defined by the RHF formalism used in calculations, is 279 kJ mol⁻¹. A similar H-bridged TS structure for the proton-transfer step in the 1,1-CH₄ elimination of CH₃CH₂O⁻ was reported.¹³ Dissociation of **12**_{imc}, formed from the incipient product pairs, leads to CH₄ and HCS⁻. The barrier to this dissociation is ca. 9 kJ mol⁻¹.

On the UMP2/6-31++G(d) PES, homolytic cleavage of the C–C bond of **1** leads to the formation of **11**_{ircx} via TS(**1**→**11**_{ircx}). Connecting **11**_{ircx} and **12**_{imc} is TS(**11**_{ircx}→**12**_{imc}). At the G2UMP2++ level, TS(**1**→**11**_{ircx}) is slightly lower in energy (by 8 kJ mol⁻¹) than **11**_{ircx}. The two-barrier pathway at the UMP2/6-31++G(d) level becomes a single-barrier one at the G2UMP2++ level, as can be seen from Figure 4b. The barrier to this homolytic pathway is 293 kJ mol⁻¹. The structure of TS(**11**_{ircx}→**12**_{imc}) is very similar to that of TS(**1**→**12**_{imc}), as shown in Figure 4a. In particular, their respective UQCISD/6-31++G(d) and RQCISD/6-31++G(d) structures suggest they are indeed the same structure. Regardless of the mode of initial bond cleavage, both (heterolytic and homolytic) pathways lead to the same TS. The complex [CH₃⁻...H₂CS] formed in the course of cleavage of the C–C bond might have a substantial mix of [CH₃⁻...H₂CS] and [CH₃...H₂CS⁻] characters since the energies of these two limiting states are quite similar. The computational approach used in this work, which is based on a single determinantal function, is certainly inadequate to characterize the nature of this kind of INC. Multiconfiguration-based methods⁷⁰ such as complete active space self-consistent field method would be required in order to properly describe the electronic structure of the system. On the other hand, when A and B have similar EAs, [A⁻...B] and [A...B⁻] often have similar energies. These factors may facilitate electron transfer between

the fragments within the INC, i.e., interconversion of [A⁻...B] and [A...B⁻].

Despite that [CH₃⁻...H₂CS⁻] and [CH₃⁻...H₂CS] have similar energies, we favor the use of the G2UMP2++ results to characterize the limiting pathway (homolytic dissociation) of reaction 11 since reaction 6 (homolytic dissociation) is energetically more favorable than reaction 5 (heterolytic dissociation).

Reaction 11 is a higher-energy (by about 33 kJ mol⁻¹) process than reaction 9. In the limiting case, initial C–C bond cleavage leads to formation of [CH₃⁻...H₂CS⁻]. The fragments of the initially formed [CH₃⁻...H₂CS⁻] rotate relative to each other to an appropriate orientation such that H transfer is possible. Subsequent H transfer takes place via TS(**11**_{ircx}→**12**_{imc}), followed by dissociation of **12**_{imc}, leading to the final elimination products.

3.5.4. 1,1-H₂ Elimination of 1 (Reaction 12). Loss of H⁻ from the methyl group of **1** leads to the formation of IMC **14**_{imc} with a cyclic neutral (Figure 5a) via TS(**1**→**13**_{imc}), **13**_{imc}, and TS(**13**_{imc}→**14**_{imc}). As can be seen from Figure 5a, the structures of TS(**1**→**13**_{imc}), **13**_{imc}, and TS(**13**_{imc}→**14**_{imc}) are IMC-like, and they have similar energies (Figure 5b). The G2++ energy barrier to the initial formation of [H⁻...c-CH₂SCH₂] **14**_{imc} is 283 kJ mol⁻¹. Three possible paths await **14**_{imc}: (i) isomerization **14**_{imc} → **14**_{imc} (migration of the hydride fragment from one CH₂ group to the other) via TS(**14**_{imc}→**14**_{imc}); (ii) proton transfer within the complex **14**_{imc} → **15**_{imc} via TS(**14**_{imc}→**15**_{imc}); and (iii) dissociation of the ion–neutral pair **14**_{imc} → H⁻ + c-CH₂-CH₂S. The last dissociation requires a critical energy of 42 kJ mol⁻¹, while the energy barrier to the proton-transfer step is 23 kJ mol⁻¹ (Figure 5b). The TS(**14**_{imc}→**15**_{imc}) is a H-bridged complex, as shown in Figure 5a. The IMC **15**_{imc} is in a potential well of 4 kJ mol⁻¹ deep relative to H₂ + c-CH₂CHS⁻. The overall energy cost for reaction 12 is 303 kJ mol⁻¹.

Since the isomerization **14**_{imc} → **14**_{imc} has a very small energy barrier (1 kJ mol⁻¹), it would occur frequently prior to dissociation of **14**_{imc} and proton transfer within the IMC. Hence, both 1,1-elimination and 1,2-elimination are operative in reaction 12.

3.6. Rearrangements of 1. Via 1,2-H shift **1** can transform into **3** via TS(**1**→**3**), which is 259 kJ mol⁻¹ above **1**. The reverse barrier is 78 kJ mol⁻¹. The energy cost of **1** → **3** is similar to that of reaction 9. It is expected that interconversion between **1** and **3** occurs to a small extent prior to fragmentations of **1** from an energetic viewpoint. Conversion of **1** to **4/5** obviously requires the rearrangement of the heavy-atom skeleton. Unlike the oxygen analogue of **1**,¹³ we found no TS for the 1,2-methyl shift. However, the conversion can also be achieved through a dissociation and recombination mechanism: **1** → [CH₃⁻...H₂CS]⁻ → **4/5**. Assuming that the association step has no or a small energy barrier and using the energy of its limiting state, [CH₃⁻...H₂CS] or [CH₃...H₂CS⁻], we estimate the energy barrier of the conversion **1** → **4/5** to be 285 kJ mol⁻¹. In summary, occurrence of rearrangements of **1** to other isomers of [C₂H₅S]⁻ prior to fragmentations of **1** is energetically plausible, though its extent may not be significant.

4. Conclusion

Among the isomers/conformers of [C₂H₅S]⁻ **1** is the lowest in energy. Its calculated Δ*H*_{f,298} (–86 kJ mol⁻¹) is in good agreement with the experimental value,²⁵ –90 kJ mol⁻¹. Contrary to its corresponding oxygen analogue, 2-mercaptoethyl anion (HSCH₂CH₂⁻) is unstable with respect to dissociation to HS⁻ + C₂H₄ without an energy barrier. β-Substituted ethyl carbanions XCH₂CH₂⁻ (e.g., X = F, SH, Cl) with EA(X) >

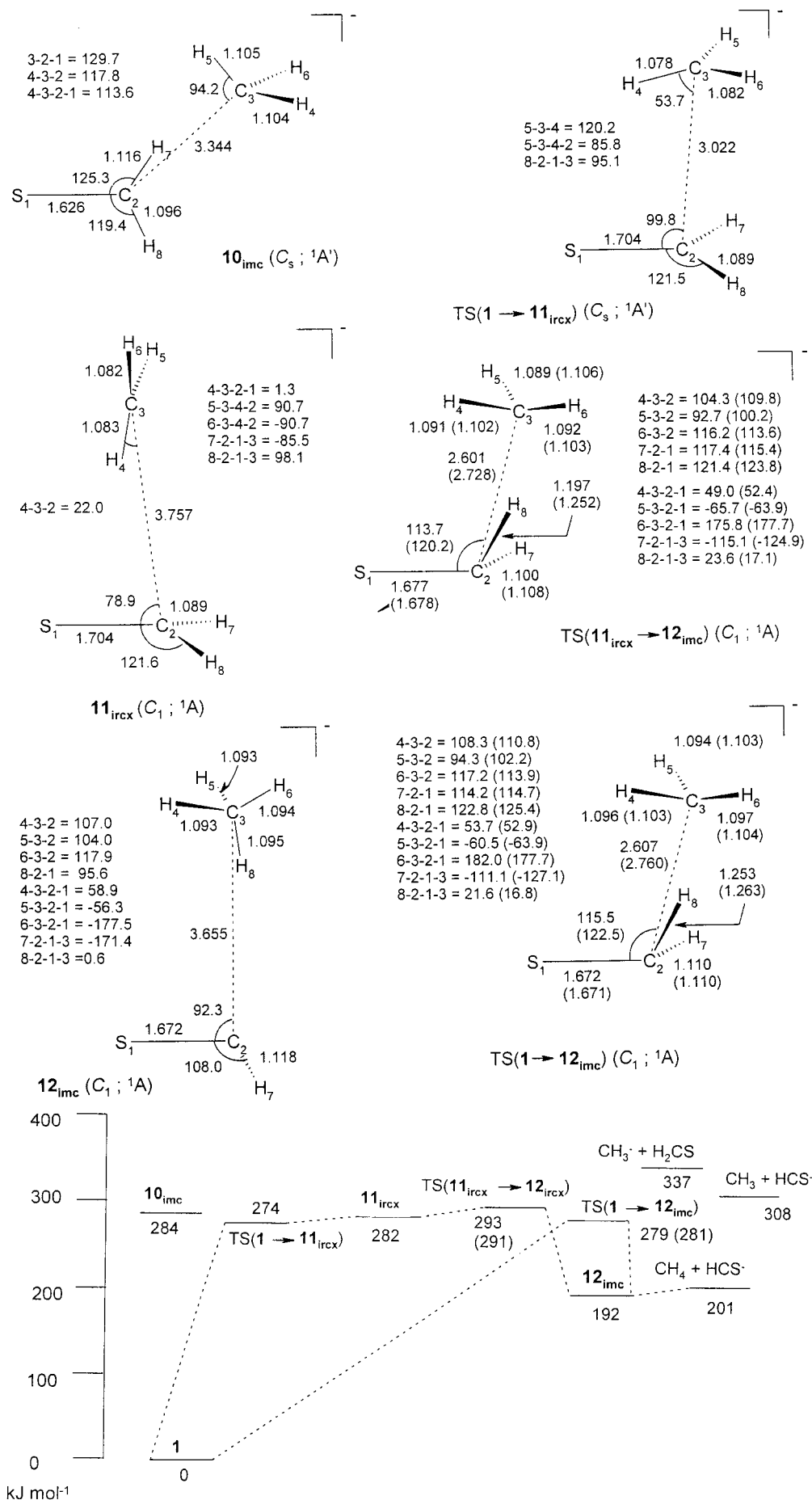
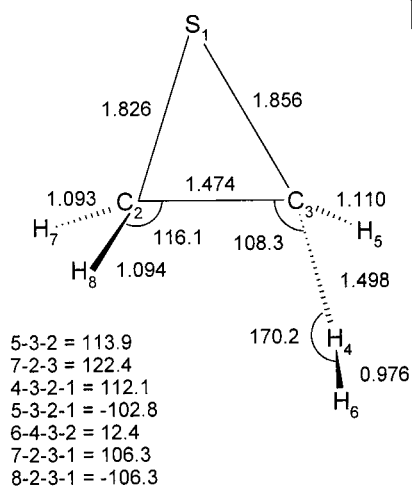
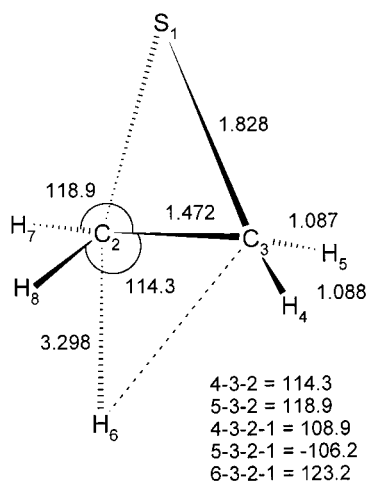
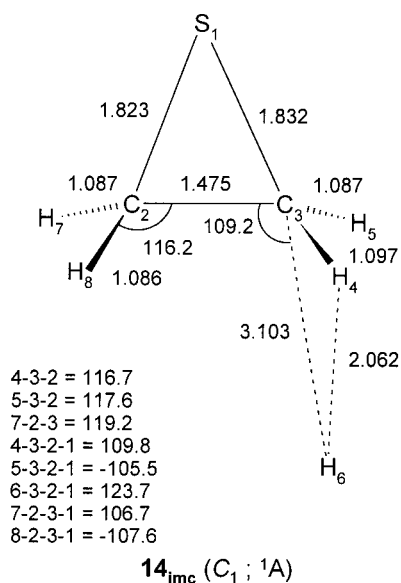
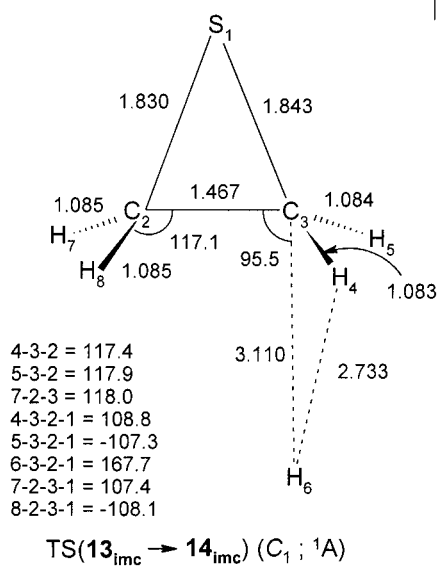
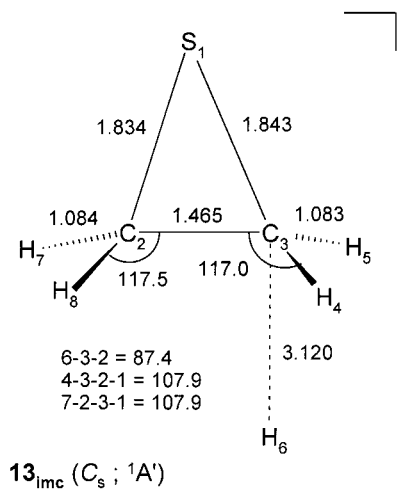
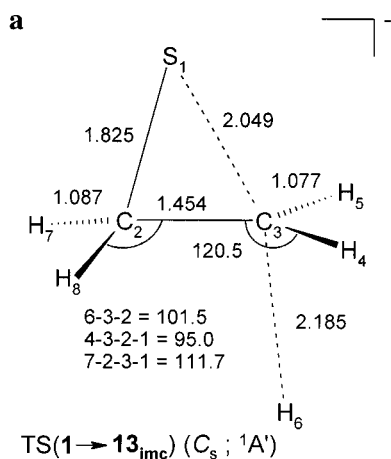


Figure 4. (a) MP2/6-31++G(d) and QCISD/6-31++G(d) optimized INC and TS structures for reaction 11. (b) Potential energy surface for reaction 11.



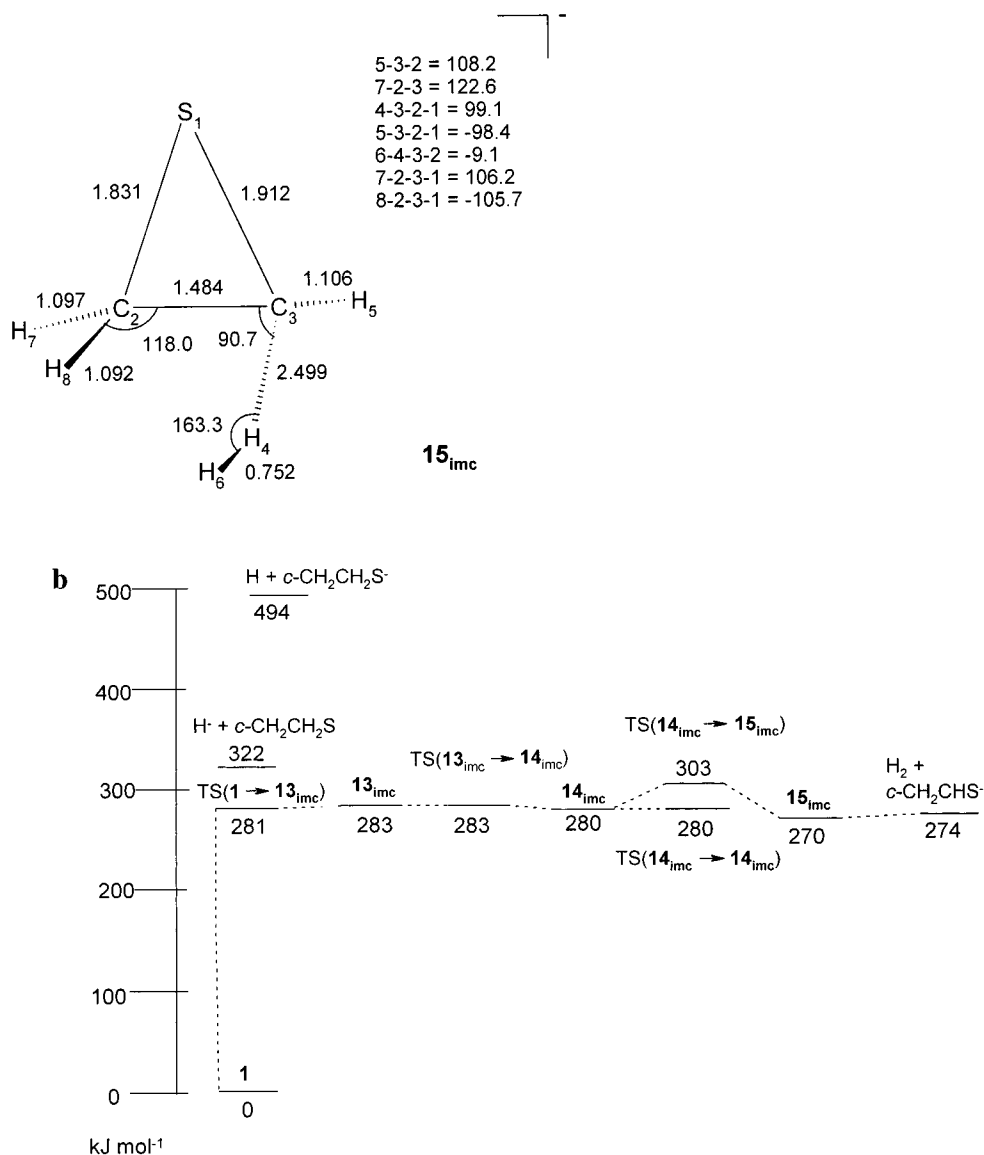


Figure 5. (a) MP2/6-31++G(d) optimized INC and TS structures for reaction 12. (b) Potential energy surface for reaction 12.

EA(OH) generally autodisproportionate to X⁻ and ethylene. The preferred conformation of the α -SR substituted carbanions studied in this work is the syn conformation. While **2**, which has a G2++ $\Delta H_{f,298}$ value of 78 kJ mol⁻¹, is lower in energy than **3** by 18 kJ mol⁻¹, **4** and **5** essentially have the same energy. Their respective $\Delta H_{f,298}$ values are 86 and 83 kJ mol⁻¹, in agreement with the observed value,²⁵ 77.4 \pm 9.2 kJ mol⁻¹, which does not distinguish between the two conformers. Interconversions between **2** and **3** as well as between **4** and **5** mainly proceed through inversion at the anionic centers. The inversion process **2** \rightarrow **3** has a barrier of 23 kJ mol⁻¹, and that for **4** \rightarrow **5** is very small (< 2 kJ mol⁻¹). The large barriers (38–47 kJ mol⁻¹) to rotation about the corresponding C α -S bonds of the HSCH₂⁻, CH₃CHSH⁻, and CH₃SCH₂⁻ indicate they have partial double character. Delocalization of the anionic lone pair into the $\sigma^*(S-R)$ orbital has some net π bonding effect between the C α and S atoms of these α -SR substituted carbanions.

Among the elimination reactions of **1** studied in this work, 1,2-H₂ (reaction 9) and 1,2-HS⁻ (reaction 10) eliminations are the most favorable energetically. The former pathway is IMC-mediated and has an energy barrier of 260 kJ mol⁻¹; the latter is IRCX-mediated with a barrier of 267 kJ mol⁻¹. Nevertheless, they are high-energy processes as compared to the 1,2-H₂

elimination of CH₃CH₂O⁻, which has an overall energy barrier¹³ of 126 kJ mol⁻¹ and is the only fragmentation pathway observed.^{1,10} Therefore, occurrence of 1,2-elimination reactions of **1** is much less probable than that of CH₃CH₂O⁻. The other two plausible 1,1-CH₄ (reaction 11) and 1,1-H₂ (reaction 12) elimination reactions of **1** have even higher energy barriers, ca. 300 kJ mol⁻¹.

Rearrangement **1** \rightarrow **3** has an energy barrier of 259 kJ mol⁻¹ and is competitive with reactions 9 and 10. Conversion of **1** to **4/5** may take place through a dissociation and recombination mechanism, and the estimated energy cost is ca. 285 kJ mol⁻¹.

Acknowledgment. The work described in this paper was partially supported by a grant from the Research Grants Council of the Hong Kong Special Administrative Region (Project No. CUHK4275/00P).

References and Notes

- (1) Mercer, R. S.; Harrison, A. G. *Can. J. Chem.* **1988**, *66*, 2947.
- (2) Raftery, M. J.; Bowie, J. H.; Sheldon, J. C. *J. Chem. Soc., Perkin Trans. 2* **1988**, 563.
- (3) Eichinger, P. C. H.; Bowie, J. H. *J. Chem. Soc., Perkin Trans. 2* **1988**, 497.

- (4) Eichinger, P. C. H.; Bowie, J. H.; Blumenthal, T. *J. Org. Chem.* **1986**, *51*, 5078.
- (5) Sheldon, J. C.; Bowie, J. H.; Lewis, D. E. *New. J. Chem.* **1988**, *12*, 269.
- (6) Tumas, W.; Foster, R. F.; Pellerite, M. J.; Brauman, J. I. *J. Am. Chem. Soc.* **1984**, *106*, 4053.
- (7) Tumas, W.; Foster, R. F.; Pellerite, M. J.; Brauman, J. I. *J. Am. Chem. Soc.* **1983**, *105*, 7464.
- (8) Hayes, R. N.; Sheldon, J. C.; Bowie, J. H.; Lewis, D. E. *Aust. J. Chem.* **1985**, *38*, 1197.
- (9) Hayes, R. N.; Sheldon, J. C.; Bowie, J. H.; Lewis, D. E. *J. Chem. Soc., Chem. Commun.* **1984**, 1431.
- (10) Tumas, W.; Foster, R. F.; Brauman, J. I. *J. Am. Chem. Soc.* **1988**, *110*, 2714.
- (11) Tumas, W.; Foster, R. F.; Pellerite, M. J.; Brauman, J. I. *J. Am. Chem. Soc.* **1987**, *109*, 961.
- (12) McAdoo, D. *J. Mass Spectrom. Rev.* **1988**, *7*, 363.
- (13) Chiu, S.-W.; Lau, K.-C.; Li, W.-K. *J. Phys. Chem. A* **1999**, *103*, 6003.
- (14) Chiu, S.-W.; Li, W.-K. Manuscript under preparation, to be published.
- (15) Frisch, M. J.; Trucks, G. W.; Schlegel, H. B.; Gill, P. M. W.; Johnson, B. J.; Robb, M. A.; Cheeseman, J. R.; Keith, T. A.; Petersson, G. A.; Montgomery, J. A.; Raghavachari, K.; Al-Laham, M. A.; Zarkewski, V. G.; Ortiz, J. V.; Foresman, J. B.; Cioslowski, J.; Stefanov, B. B.; Nanayakkara, A.; Challacombe, M.; Peng, C. Y.; Ayala, P. Y.; Chen, W.; Wong, M. W.; Andres, J. L.; Replogle, E. S.; Gomperts, R.; Martin, R. L.; Fox, D. J.; Binkley, J. S.; Defrees, D. J.; Baker, J.; Stewart, J. J. P.; Head-Gordon, M.; Gonzalez, C.; Pople, J. A. *GAUSSIAN 94*, Revision D4; Gaussian, Inc.: Pittsburgh, PA, 1995.
- (16) Frisch, M. J.; Trucks, G. W.; Schlegel, H. B.; Scuseria, G. E.; Robb, M. A.; Cheeseman, J. R.; Zakrzewski, V. G.; Montgomery, J. A., Jr.; Stratmann, R. E.; Burant, J. C.; Dapprich, S.; Millam, J. M.; Daniels, A. D.; Kudin, K. N.; Strain, M. C.; Farkas, O.; Tomasi, J.; Barone, V.; Cossi, M.; Cammi, R.; Mennucci, B.; Pomelli, C.; Adamo, C.; Clifford, S.; Ochterski, J.; Petersson, G. A.; Ayala, P. Y.; Cui, Q.; Morokuma, K.; Malick, D. K.; Rabuck, A. D.; Raghavachari, K.; Foresman, J. B.; Cioslowski, J.; Ortiz, J. V.; Baboul, A. G.; Stefanov, B. B.; Liu, G.; Liashenko, A.; Piskorz, P.; Komaromi, I.; Gomperts, R.; Martin, R. L.; Fox, D. J.; Keith, T.; Al-Laham, M. A.; Peng, C. Y.; Nanayakkara, A.; Gonzalez, C.; Challacombe, M.; Gill, P. M. W.; Johnson, B.; Chen, W.; Wong, M. W.; Andres, J. L.; Gonzalez, C.; Head-Gordon, M.; Replogle, E. S.; Pople, J. A. *GAUSSIAN 98*, Revision A.7; Gaussian, Inc.: Pittsburgh, PA, 1998.
- (17) For a recent reference on the scaling factors for zero-point energy and thermal correction, see, for example: Scott, A. P.; Radom, L. *J. Phys. Chem.* **1996**, *100*, 16502.
- (18) Gonzalez, C.; Schlegel, H. B. *J. Chem. Phys.* **1989**, *90*, 2154.
- (19) Gonzalez, C.; Schlegel, H. B. *J. Phys. Chem.* **1990**, *94*, 5523.
- (20) Chiu, S.-W.; Lau, K.-C.; Li, W.-K.; Ma, N. L.; Cheung, Y.-S.; Ng, C. Y. *J. Mol. Struct. (THEOCHEM)* **1999**, *490*, 109.
- (21) Chiu, S.-W.; Lau, K.-C.; Li, W.-K. *J. Phys. Chem. A* **2000**, *104*, 3028.
- (22) Chiu, S.-W.; Cheung, Y.-S.; Ma, N. L.; Li, W.-K.; Ng, C. Y. *J. Mol. Struct. (THEOCHEM)* **1998**, *452*, 97.
- (23) Chiu, S.-W.; Cheung, Y.-S.; Ma, N. L.; Li, W.-K.; Ng, C. Y. *J. Mol. Struct. (THEOCHEM)* **1999**, *468*, 21.
- (24) Jarzecki, A.; Davidson, E. R. *J. Phys. Chem. A* **1998**, *102*, 4742.
- (25) Afeefy, H. Y.; Liebman, J. F.; Stein, S. E. Neutral Thermochemical Data. In *NIST Chemistry WebBook*; Mallard, W. G., Linstrom, P. J., Eds.; NIST Standard Reference Database No. 69; National Institute of Standards and Technology: Gaithersburg MD, 2000; p 20899 and references therein (<http://webbook.nist.gov>).
- (26) Curtiss, L. A.; Raghavachari, K.; Trucks, G. W.; Pople, J. A. *J. Chem. Phys.* **1991**, *94*, 7221.
- (27) Moran, S.; Ellison, G. B. *Int. J. Mass Spectrom. Ion Processes* **1987**, *80*, 83.
- (28) Ruscic, B.; Berkowitz, J. *J. Chem. Phys.* **1993**, *98*, 2568.
- (29) Chiu, S.-W.; Cheung, Y.-S.; Ma, N. L.; Li, W.-K.; Ng, C. Y. *J. Mol. Struct. (THEOCHEM)* **1997**, *397*, 87.
- (30) Moran, S.; Ellison, G. B. *J. Phys. Chem.* **1988**, *92*, 1794.
- (31) Janousek, B. K.; Reed, K. J.; Brauman, J. I. *J. Am. Chem. Soc.* **1980**, *102*, 3125.
- (32) Hudson, R. F.; Eisenstein, O.; Anh, N. T. *Tetrahedron* **1975**, *31*, 751.
- (33) DeFrees, D. J.; Bartness, J. E.; Kim, J. K.; McIver, R. T., Jr.; Hehre, W. J. *J. Am. Chem. Soc.* **1977**, *99*, 6451.
- (34) Pross, A.; Radom, L. *J. Am. Chem. Soc.* **1978**, *100*, 6572.
- (35) Chiu, S.-W.; Li, W.-K.; Tseng, W.-B.; Ng, C. Y. *J. Chem. Phys.* **1992**, *97*, 6557.
- (36) Cheung, Y.-S.; Li, W.-K.; Ng, C. Y. *J. Mol. Struct. (THEOCHEM)* **1995**, *339*, 25.
- (37) Wiberg, K. B.; Castejon, H. *J. Am. Chem. Soc.* **1994**, *116*, 10489.
- (38) Epiotis, N. D.; Yates, R. L.; Bernardi, F.; Wolfe, S. *J. Am. Chem. Soc.* **1976**, *98*, 5435.
- (39) (a) Wolfe, S.; LaJohn, L. A.; Bernardi, F.; Mangini, A.; Tonachini, F. *Tetrahedron Lett.* **1983**, *24*, 3789. (b) Wolfe, S.; Stolow, A.; LaJohn, L. A. *Tetrahedron Lett.* **1983**, *24*, 4071.
- (40) Holtz, D. *Prog. Phys. Org. Chem.* **1971**, *8*, 1.
- (41) (a) Foster, J. P.; Weinhold, F. *J. Am. Chem. Soc.* **1980**, *102*, 7211. (b) Reed, A. E.; Weinhold, F. *J. Chem. Phys.* **1983**, *78*, 4066. (c) Reed, A. E.; Weinstock, R. B.; Weinhold, F. *J. Chem. Phys.* **1985**, *83*, 735. (d) Reed, A. E.; Weinhold, F.; Curtiss, L. A.; Pochatko, D. J. *J. Chem. Phys.* **1986**, *84*, 5687. (e) Reed, A. E.; Curtiss, L. A.; Weinhold, F. *Chem. Rev.* **1988**, *88*, 899.
- (42) Bernardi, F.; Bottoni, A.; Venturini, A.; Mangini, A. *J. Am. Chem. Soc.* **1986**, *108*, 8171.
- (43) Lehn, J.-M.; Wipff, G. *J. Am. Chem. Soc.* **1976**, *98*, 7498.
- (44) Borden, W. T.; Davidson, E. R.; Andersen, N. H.; Denniston, A. D.; Epiotis, N. D. *Am. Chem. Soc.* **1978**, *100*, 1604.
- (45) Schleyer, P. v. R.; Kos, A. *J. Tetrahedron* **1983**, *39*, 1141.
- (46) Roy, M.; McMahon, T. B. *Can. J. Chem.* **1985**, *63*, 708.
- (47) Nobes, R. H.; Poppinger, D.; Li, W.-K.; Radom, L. In *Comprehensive Carbanion Chemistry, Part C*; Buncl, E., Durst, T., Eds.; Elsevier: Amsterdam, 1987.
- (48) Moylan, C. R.; Brauman, J. I. *J. Am. Chem. Soc.* **1985**, *107*, 761.
- (49) Audier, H. E.; Bouchoux, G.; McMahon, T. B.; Milliet, A.; Vulpius, T. *Org. Mass Spectrom.* **1994**, *29*, 176.
- (50) Nguyen, M. T.; Bouchoux, G. *J. Phys. Chem.* **1996**, *100*, 2089.
- (51) Wang, D.; Squires, R. B. *Int. J. Mass Spectrom. Ion Processes* **1991**, *107*, R7.
- (52) Heinrich, N.; Louage, F.; Lifshitz, C.; Schwarz, H. *J. Am. Chem. Soc.* **1988**, *110*, 8183.
- (53) Morton, T. H. *Org. Mass Spectrom.* **1992**, *27*, 353.
- (54) Bowen, R. D. *Acc. Chem. Res.* **1991**, *24*, 364.
- (55) Langford, C. H.; Gray, H. B. *Ligand Substitution Processes*; Benjamin: New York, 1965.
- (56) Chronister, E. L.; Morton, T. H. *J. Am. Chem. Soc.* **1990**, *112*, 133.
- (57) Chesnavich, W. J.; Bowers, M. T. *J. Chem. Phys.* **1985**, *82*, 65.
- (58) Truhlar, D. G. *J. Chem. Phys.* **1985**, *82*, 2166.
- (59) Chesnavich, W. J. *J. Chem. Phys.* **1986**, *84*, 2615.
- (60) Dodd, J. A.; Golden, D. M.; Brauman, J. I. *J. Chem. Phys.* **1984**, *80*, 1894.
- (61) Dodd, J. A.; Golden, D. M.; Brauman, J. I. *J. Chem. Phys.* **1985**, *82*, 2169.
- (62) McAdoo, D. J.; Traeger, J. C.; Hudson, C. E.; Griffin, L. L. *J. Chem. Phys.* **1988**, *92*, 9524.
- (63) Kebarle, P. *Annu. Rev. Phys. Chem.* **1977**, *28*, 445.
- (64) I. S. Hammerum, M. M. Hansen, H. E. Audier, *Int. J. Mass Spectrom.* **1977**, *160*, 183.
- (65) Melander, L.; Saunders, W. H. *Reactions of Isotopic Molecules*; Wiley: New York, 1980.
- (66) Wong, M. W.; Baker, J.; Nobes, R. H.; Radom, L. *J. Am. Chem. Soc.* **1987**, *109*, 2245.
- (67) Gill, P. M. W.; Wong, M. H.; Nobes, R. H.; Radom, L. *Chem. Phys. Lett.* **1988**, *148*, 541.
- (68) Gill, P. M. W.; Radom, L. *Chem. Phys. Lett.* **1986**, *132*, 16.
- (69) Carsky, P.; Hubak, E. *Theo. Chim. Acta* **1991**, *80*, 407.
- (70) (a) Roos, B. O. The Complete Active Space Self-consistent Field Method and Its Applications in Electronic Structure Calculations. In *Advances in Chemical Physics: Ab Initio Methods in Quantum Chemistry - II*; Lawley, K. P., Ed.; Wiley: Chichester, England, 1987; p 399. (b) Andersson, K.; Malmqvist, P.-Å.; Roos, B. O. *J. Chem. Phys.* **1992**, *96*, 1218. (c) Roos, B. O.; Andersson, K.; Fülscher, M. P.; Malmqvist, P.-Å.; Serrano-Andrés, L.; Pierloot, K.; Merchán, M. Multiconfigurational Perturbation Theory: Applications in Electronic Spectroscopy. In *Advances in Chemical Physics: New Methods in Computational Quantum Mechanics*; Prigogine, I., Rice, S. A., Eds.; Wiley: New York, 1996; Vol. XCIII, p 219.
- (71) Lias, L. G.; Bartmess, E.; Lieman, J. F.; Holmes, J. L.; Levin, L. D.; Mallard, W. D. *J. Phys. Chem. Ref. Data* **1988**, *17* (Suppl. 1).